

# Mars Libration Point Mission Simulations

Jon D. Strizzi; Joshua M. Kutrieb; Paul E. Damphousse; John P. Carrico  
[2001]

## Abstract

The equilibrium points of the Sun-Mars system bring some unique characteristics to the discussion of future inner solar system exploration missions, particularly an expedition to Mars itself. Existing research has identified potential utility for Sun-Mars libration point missions, particularly for satellites orbiting each of the co-linear, near-Mars, Sun-Mars libration points (the  $L_1$  and  $L_2$  points) serving as Earth-Mars communication relays. Regarding these Lissajous orbits, we address questions of “Why go there?” “How to get there?” and “How to stay there?” Namely, we address utility and usefulness, transfer and injection, and station-keeping. The restricted 3-body problem involving a spacecraft in that system is reviewed; and past and present research and proposals involving the use of these orbits are summarized and discussed. We use commercial, desktop tools (Satellite Tool Kit (STK) / *Astrogator*) for simulation and analysis of Earth-Mars transfers, Lissajous orbit insertions, and station-keeping trajectories. On-going, successful collaboration between military and industry researchers in a virtual environment is demonstrated. Much of this study focuses on 2016 Earth-Mars transfers to these mission orbits with their trajectory characteristics and sensitivities. This includes analysis of using a mid-course correction as well as a braking maneuver at close approach to Mars to control Lissajous orbit insertion and the critical parameter of the phasing of the two-vehicle relay system. Station-keeping sensitivities are investigated via a Monte Carlo technique. The resulting data provides confirmation and insight for existing research and proposals, as well as new information on Mars transfer and Lissajous orbit insertion strategies, communications coverage, and station-keeping sensitivities. The data provides new information on these trajectories to future researchers and mission planners

## Introduction

*“NASA’s vision is to . . . focus more of our energy on going to Mars and beyond.”*

— Dan Goldin, AWST, January 2001

*“All the questions we have about Mars could now be answered . . . if we could just walk around on the planet for a few days.”*

— Michael Malin, Malin Space Science Systems, National Geographic, February 2001

*“NASA is seeking innovation to attack the diversity of Mars . . . to change the vantage point from which we explore . . .”*

— CNN, June 2001

As NASA and the space community renew their focus on Mars exploration, student researchers find several topics awaiting further study. From our work that originated in an advanced astrodynamics course at the US Naval Postgraduate School, we became interested in Mars, various aspects of the three-body problem, and the Lagrange or libration points, and we were eager to team with industry to conduct mission simulations and analysis. We examined several documented research efforts dealing with diverse aspects of these topics.<sup>6,9,11,14,19,20,24,25</sup> The concept of using communication relay vehicles in orbit about colinear Lagrange points to support exploration of the secondary body is not entirely new, being first conceptualized in the case of the Earth-Moon system by R. Farquhar.<sup>24,25</sup> An innovative approach on the concept that caught our interest was that introduced by H. Pernicka, et al, for a 2-satellite communications relay with one spacecraft in orbit about each of the co-linear, near Mars, Sun-Mars libration points,  $L_1$  and  $L_2$ .<sup>6</sup> Further work by graduate researchers (Kok-Fai Tai and Danehy) refined this proposal and conducted investigations into the technical and fiscal aspects of such a mission, including trade studies on communication relay constellation options.<sup>15,16</sup> This analysis resulted in some favorable conclusions and rationale for a Mars communication relay system that utilizes 2-spacecraft in large amplitude Lissajous orbits, including system cost and performance measures comparable to a 3-spacecraft aerosynchronous system.

A primary purpose of this work, then, was to re-examine the 2-vehicle system orbiting the Sun-Mars co-linear libration points, including transfer orbits and station-keeping, through desktop computer simulation using full-force models and the interplanetary propagation / targeting techniques of the STK / *Astrogator* module. Essentially, we wished to see how past studies and data using simplified models compared to our new full-force model targeting and propagation, and to generate innovative scenarios and data for future missions.

An additional purpose of the project was to demonstrate successful collaboration between military graduate researchers and industry professionals. Timely, affordable results from specific research can be obtained when diverse groups such as these can work, virtually and collaboratively, on pieces of a complex problem. These ideas flow into another purpose of the study: to show how commercial desktop computing can be used to easily create and analyze these types of missions and problems, again leading to faster and cheaper studies by more researchers. As far as we could determine, this area of study for Mars missions has not been investigated previously in this manner.

As output for this study, we expand upon discussions of the usefulness of these orbits for Mars missions as well as re-examine the 2003 Earth-Mars transfers and L1 libration orbit insertions presented in the original Pernicka study and the follow-on work. We then expand that simulation and analysis to include the planning horizon of a 2016 transfer and mission orbit insertion, considering an L2 orbit insertion as well. We investigate the effects of orbit amplitude on insertion  $\Delta V$  requirements and show some innovative mission orbit insertion techniques that results in  $\Delta V$  savings, namely using a Mars swingby and braking maneuver to assist in the insertion. We also investigate trajectory design methods to achieve the necessary two-vehicle phasing for effective mission operations. We present figures of merit to assess the communications relay coverage and analyze station-keeping  $\Delta V$  requirements via Monte Carlo simulation and analysis.

Please note that this report consolidates and expands upon some results presented at American Institute of Aeronautics and Astronautics and American Astronautical Society conferences,<sup>22,23</sup> along with additional explanatory material. All of the simulation and analysis presented here represents a first effort of utilizing full force models and current desktop computing tools to generate some useful data on the Sun-Mars libration point transfer and communication relay problem. The data does not represent optimized numerical solutions or proposed detailed mission designs, but rather information and baseline data for follow-on researchers and mission planners.

**Background: The Three-Body Problem and Libration Points** <sup>3,4,7</sup>

A standard simplified approach for initial investigations into interplanetary trajectories relies on reducing a complex “four-body” problem (Sun, Earth, Planet, and Spacecraft) down to three phases of simplified “two-body” problems (Primary body and Spacecraft). These are usually identified as the departure, cruise, and arrival phases, and this approximate solution approach is typically called the “patched conic approach.” A general picture of this is depicted in Figure 1 for a transfer from Earth to another planet (in this case, an inner planet and not Mars). The “spheres of influence” mark the boundaries for the phases of the trajectories.

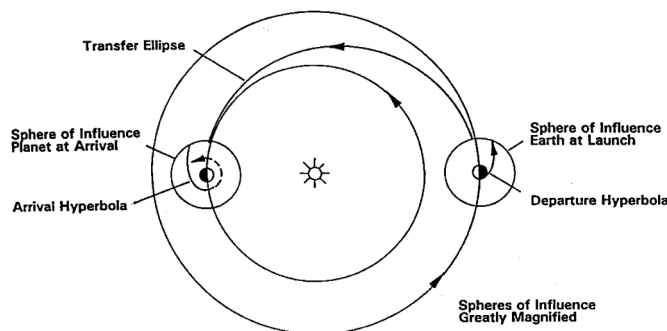


Figure 1. Spheres of Influence for Patched Conic Trajectories

To consider trajectories to and orbits about the libration points, one must address the “three body problem,” which involves two primary masses and a much smaller third mass (the spacecraft). There is some history behind the search

for analytic solutions to this problem involving some rather well known figures. Newton tackled some aspects of this problem when he computed the orbit of the moon to within 8% in 1687. Euler developed his problem of “two fixed force centers” in 1760 and the rotating / synodic coordinate system in 1772. Jacobi created his integral solutions from the Euler “restricted” three-body system in 1772. That same year, Lagrange identified the “equilibrium” points of a restricted three-body system. These points (there are five in all) have since been labeled “Lagrange points” and are also known as “libration points.” Orbits about these points in space are termed “libration orbits” or “Lissajous orbits.” A specific type of Lissajous orbit is often called a “halo orbit.”

The five libration points are defined in a rotating coordinate frame in which 2 large primary bodies rotate about their common center of mass. Looking “down” upon the plane of rotation of these two bodies, these points can be labeled as in Figure 2.

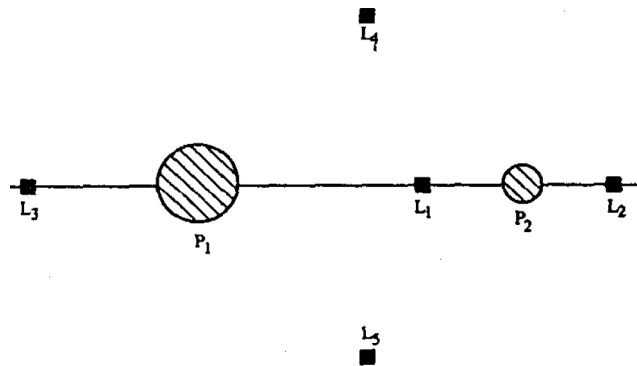


Figure 2. Geometry of the Lagrange Points of Two Primary Masses  $P_1$  and  $P_2$ <sup>7</sup>

The resulting motion and force balancing in this synodic frame produces the five equilibrium points, where a third body of small relative mass would theoretically remain once placed there. The points numbered 1, 2, and 3 are termed the collinear points since they lie on the line connecting the two primary bodies, and are unstable in the sense that an object placed there will eventually depart due to the unstable nature and disturbance forces. Points 4 and 5 are the triangular points since lines connecting them to the primaries form equilateral triangles, and are stable. A way to envision this system of points is that of energy balancing, where the collinear points represent balancing on the top of a “peak” and the triangular points represent balancing in the trough of a “valley.” Fairly stable use of the collinear points can be achieved by placing an object in orbit about the points. It is also interesting to note that the existence of these equilibrium points, as predicted by Lagrange in 1772, were finally confirmed 134 years later by the discovery of the so-called “Trojan” asteroids, which are objects that have collected near the Sun-Jupiter triangular points.

### A Note on Historical Missions Using Libration Points

It is important to note that there have been successful space missions utilizing libration point orbits. The first proposal for such a mission was in 1966 when John Breakwell and Robert Farquhar proposed that a satellite orbiting about the Earth-Moon  $L_2$  point could provide a communications link to support exploration of the “dark side” of the moon (more accurately referred to as the “far side”). They developed a periodic, out of plane solution for the spacecraft orbit that led to the development of halo orbits.

The first true mission into one of these orbits was the International Sun-Earth Explorer-3 (ISEE-3), launched in 1978 for operations about the Sun-Earth  $L_1$  point. Its trajectories are represented in Figure 3 and are indicative of some of the complex dynamics involved in these types of missions.

## Mars Libration Point Mission Simulations

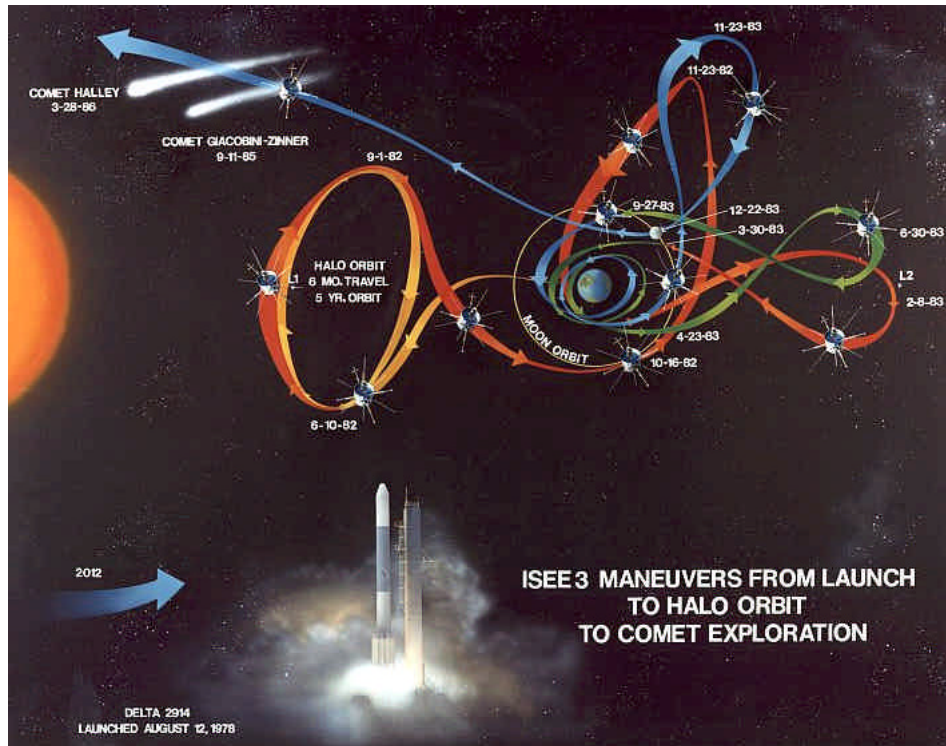


Figure 3. ISEE-3 Trajectory Summary

Another successful mission of note was the Solar and Heliospheric Observatory (SOHO) launched in 1995, which provided an unobstructed view of the Sun from its orbit about the Sun-Earth L1 point. The schematic is shown in Figure 4.

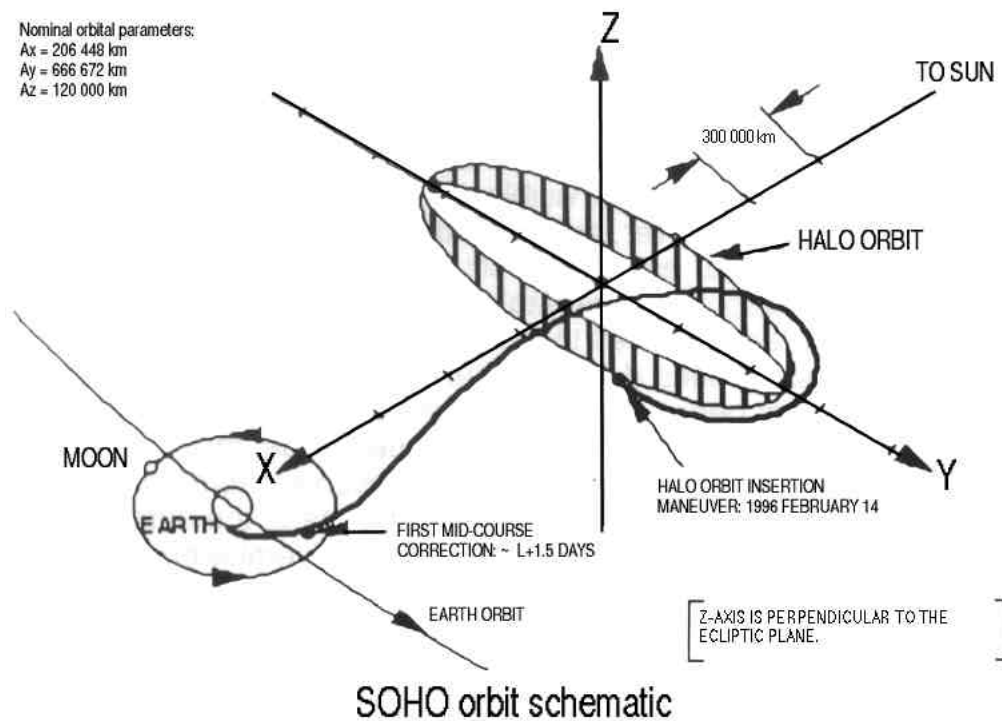


Figure 4. SOHO Trajectory Summary

There have of course been other missions since these times, but these represent some of the first successes and have paved the way for expanding upon the use of these types of orbits. There have been no missions associated with the Sun-Mars libration points to date.

### **Mars Communication Constellations**

Currently, spacecraft missions to Mars rely on their on-board equipment to provide faint transmissions directly to Earth or to a relay in Martian orbit. The addition of on-board communication equipment capable of reaching out through the interplanetary void between Mars and the Earth adds weight, cost, and risk to missions that operate within tight margins in these areas. To exacerbate this problem, once a lander has made it safely to the surface, it can only relay information to Earth when it is in direct line of sight. With a Martian day of just over 24 hours, there exist well over 12 hours of “blackout” where no signal can be sent to the Earth. With the addition of an orbiting relay, these times are reduced substantially but significant blackouts will still exist. In order to provide continuous coverage for the entire Martian surface, a minimum of four satellites (in elliptical orbits) are required.<sup>6</sup> This, once again, raises the issues of cost and risk.

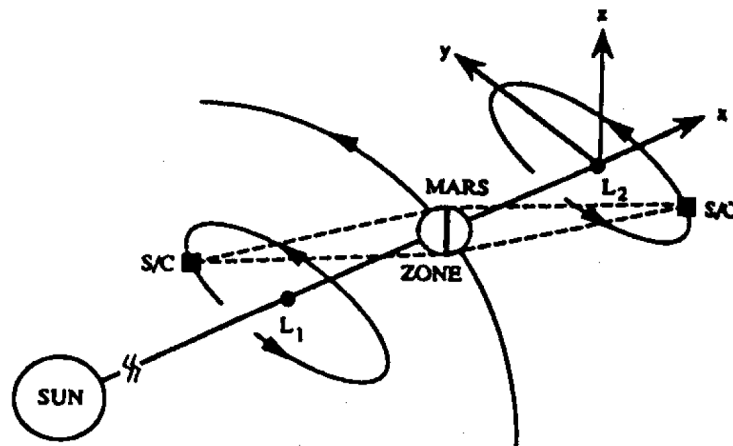
Some of these problems can be solved by the use of a communication network around Mars that takes advantage of the geometry provided by placement at the Sun-Mars Lagrange points. A minimum of two satellites located at the Sun-Mars L1 and L2 points could provide near continuous coverage for multiple vehicles on the surface and in orbit.<sup>6</sup> These points are termed the co-linear, near-Mars, Sun-Mars Libration points and are defined as above in a three-body orbital system where the two primaries are the Sun and Mars and the much smaller body is the orbiting communication relay. Note also that the Lagrange points remain at the same relative locations as the two primary bodies rotate about their center of mass. The communication satellites would be inserted into large amplitude orbits about the L1 and L2 points, circling their respective Lagrange points and the Sun-Mars line. These satellites could communicate with landers anywhere on the Martian surface, with any spacecraft in Martian orbit, and provide the critical communications link between the Earth and Mars.<sup>6</sup>

Other constellations could be used for a Mars communications network, but each has disadvantages that outweigh the advantages.<sup>16</sup> A group (four to six) of low to medium orbiting relay satellites would ensure that every satellite would cover the entire planet at some point, but the cost and risk of inserting so many satellites and the limited instantaneous field of view the satellites can offer do not make it an attractive option. Four satellites in common-period, inclined orbits, or a Draim constellation, could cover the entire surface of Mars, but again require twice as many satellites as the Lissajous orbit concept, as well as the added complexity of a ground station continuously switching from one satellite to another. An aerosynchronous constellation (like Earth geosynchronous but at Mars, approximately 20,462 km altitude) requires three or four satellites, and works well with ground stations that can simply point to one spot in the sky. However, in addition to the fact more than two satellites are required, there is virtually no polar coverage. Another proposal places communication landers on the Martian moons of Phobos and/or Deimos, but this constellation has the same inefficiencies as the aerosynchronous satellites with large gaps of polar coverage.

The L1 and L2 orbit constellation requires only two satellites for a fully operational constellation (each spacecraft sees almost half of Mars at all times), thus making it the most attractive option. The Sun is always visible to both satellites, greatly simplifying power requirements for that spacecraft. Lander pointing requirements are simple, given the spacecraft is always the same relative distance from the Sun-Mars line, and the spacecraft station-keeping budget is relatively small. Disadvantages are overcoming the approximate one million kilometer distance from the Lagrange points to the Martian surface. This distance likely requires a large, high frequency antenna, which could complicate solar panel design to minimize antenna shadow and may require a more complex lander communication system to interact with the high frequency signals. Interference from constant solar radiation along the Sun-Mars line and for a particular Earth viewing geometry may also have to be considered, and the loss of one satellite means half the planet loses communications coverage for approximately 12 hours.

Please note that this study does not attempt to address any issues related to communication link specifications or performance, but does focus on the trajectory designs to place communication relay vehicles into their mission orbits.

## Sun-Mars Libration Point Orbits

Figure 5. Sun-Mars L1 and L2 Halo Orbit Constellation<sup>6</sup>

The design of the halo orbit communication network around Mars is a simple but elegant one, as depicted in Figure 5.<sup>6</sup> In order to prevent an unneeded overlap of coverage, the orbits of each satellite at L1 and L2 would be opposed by 180 degrees but moving in the same orbital direction. Herein lies a minor problem with this configuration: because L1 and L2 are at finite distances from Mars ( $1 \times 10^6$  km), the actual view of Mars is slightly less than hemispherical. Despite this geometry, the original study predicted that the network would be able to view 99.81% of the planet at all times. The “down time” in this scenario would be minimal: a vehicle caught in this band would have to wait a mere 1.5 minutes before coverage would be switched over and reestablished with the other satellite.

In designing the proper orbits in which to place the two satellites, the most important consideration is that they permit efficient maintenance of the 180 degree offset.<sup>6</sup> An additional consideration is that of avoiding having the satellite cross what is known as the “solar exclusion zone,” the line between Mars and the Sun. Passing through this zone, communications would be disrupted due to intense solar interference. To avoid this problem the orbit must be large enough to avoid this crossing; an orbit of period greater than 0.9 years should suffice. Another obvious consideration is the choice of geometry and size of the orbit that reduces the required insertion maneuvers, and thus cost, from Earth.

As an aside, one might wonder if the L4 and L5 points could play some role in the design of a communication network around Mars. The L4 and L5 Lagrange points lead and trail Mars by 60 degrees in its orbit, thus forming equilateral triangles with Mars and the Sun (see Figure 2). The distance from Mars to either of these two Lagrange points is the same as the distance from Mars to the Sun ( $227.9 \times 10^6$  km). To communicate over these distances, current interplanetary missions use very large dishes, such as the Goldstone Deep Space Network (DSN) facility in California, in order to eliminate the need for large, powerful transceivers on the spacecraft itself. Links over this 230 million kilometer range would require space borne communications elements whose size, weight, and power would be on the order of a DSN ground station. The size and power of the needed equipment for these distances make the L4 and L5 unrealistic as locations for the network.<sup>8</sup>

There is one other interesting aspect of the L4 and L5 points worth mentioning here. While their stability can be exploited for use in missions that require minimal station-keeping, this same stability also attracts a multitude of interplanetary bodies that populate this region of the solar system. These special bodies are known as “Trojans” because the first few such objects discovered were named for several heroes from the Trojan War. By convention established by the International Astronomical Union, all similar objects must be named after Trojan War heroes, Greeks ahead of the planet and Trojans trailing the planet. Two of the larger Martian Trojans (in the 1-2 km range), 5261 Eureka and 1998 VF31, represent what could be thousands of other bodies that reside at the L4 and L5 points making these fairly dangerous places indeed. Consideration must be made as to whether the benefits of the inherent stability of the L4 and L5 points outweigh the risks of residing there.<sup>8</sup>

### **Mars L1 and L2 Constellation Advantages**

Probably the most significant advantage to using the large amplitude Lissajous orbit constellation is minimum cost associated with only 2 spacecraft required, when compared to other constellation options.<sup>15,16</sup> Additionally, spacecraft orbiting about L1 and L2 can readily see the Sun and Earth, potentially simplifying spacecraft solar cell placement and communication antenna design.

The vehicles circling the Sun-Mars L1 and L2 points will orbit the Sun-Mars line with periods on the order of 1 year. The long period dynamics of such orbits may make them attractive for interplanetary missions with significant communication time delays. Perhaps even more significantly, on a given day (or series of days) the relay vehicle will appear motionless and remain in a fixed position relative to the sun (or local midnight vector, for the L2 relay). Thus, a communication relay tracking system for explorers on the surface could be simplified and automated for tracking of this position in the sky. From the surface, there would be only one switch between relay vehicles each day, a distinct advantage over Draim or low orbiting concepts. The Sun-line geometry may also allow for simplified and robust safe-modes for the vehicles based on the sun vector. Since both spacecraft orbit about the Sun-Mars line in large amplitude Lissajous orbits and avoid eclipsing, the relays would always have access to the sun for their solar cells, thus allowing reduced battery sizes.

An additional benefit of the unique geometry offered by Lissajous orbit missions is a secondary mission for these communications relay vehicles as observation platforms. The L1 satellite is able to perform continuous solar activity monitoring via a secondary payload on the vehicle, and thus provide advance warning of activity to Mars surface missions. This could be done using low power, simple instruments for simple early warning of solar storms / flares, perhaps derived from legacy missions. Regular monitoring of the sun is thus possible, and can additionally be compared to solar data from sensors closer to the sun. This secondary mission for solar activity monitoring increases in importance when the Earth is on the opposite side of the solar system from Mars. Another observation mission for both spacecraft could include Martian weather sensing and relay to Mars expeditions and Earth. The L2 vehicle offers the opportunity of a secondary payload for asteroid and outer solar system observations.

One of the fundamental advantages of Lissajous orbit is, of course, the relatively small  $\Delta V$  maneuvers required for station-keeping, when compared to other mission orbits. Annual  $\Delta V$ s for each vehicle could be on the order of 2 m/s<sup>14</sup> and studies have produced data showing annual vehicle station-keeping estimates of 50 m/s for low orbits, almost 200 m/s for aerosynchronous, and 30 m/s for the inclined common period missions.<sup>15</sup> We provide more discussion of station-keeping in a later section of this report.

### **Mars Mission Simulations and Analysis**

#### **Satellite Tool Kit (STK) / Astrogator<sup>26</sup>**

STK / Astrogator was the simulation and analysis tool used to generate the data for this study of utilizing the Sun-Mars libration point for orbiting communication relays. This is an interactive orbit maneuver and space mission planning tool that is fully integrated within the larger STK tool and is widely used for Earth orbiting, Lunar, libration point, and interplanetary missions. The key features of this tool are the use of user-defined gravity fields, propagators, and coordinate systems. It also uses a powerful “targeted trajectory” design process and features a variety of on-line help features.

On a historical note, Astrogator has its roots in a tool called *Swingby*, which was developed by Computer Sciences Corporation (CSC) in 1989 for NASA Goddard Spaceflight Center (GSFS). This was commercialized as *Navigator* by CSC in 1994. In turn, the *Navigator* tool was purchased by Analytical Graphics, Inc. (AGI), the developers of STK. In response to GSFS requests for COTS products, *Astrogator* was developed in 1997 using some heritage algorithms from *Swingby* and *Navigator*.

For designing libration orbit missions, there are some specific tools within the Astrogator module which are employed. One of these is the rotating libration point (RLP) coordinate system. This is defined for a system of primary and less-massive secondary gravitating bodies as shown in Figure 6.

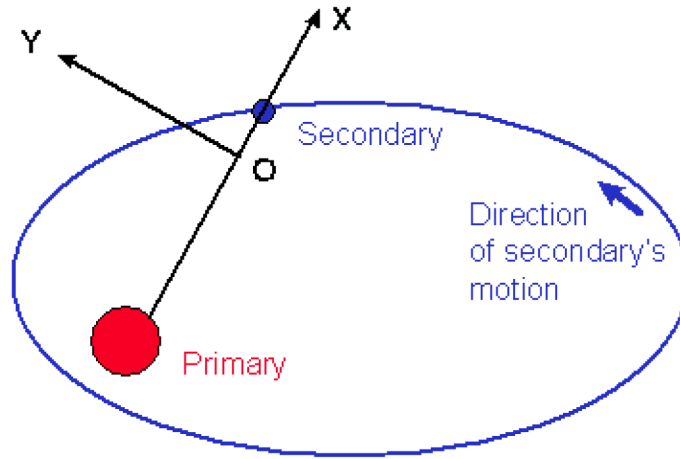


Figure 6. RLP Coordinate System<sup>26</sup>

The origin is placed at the libration point of interest. The x-axis defines the line from the primary to the secondary body (in this specific case, from the Sun to Mars). The y-axis is orthogonal to the x-axis in the plane and direction of the secondary body's motion about the primary. The z-axis completes the orthogonal set to x and y.

For velocity change ( $\Delta V$ ) computations, the velocity-normal-conormal (VNC) frame is used (see Figure 7). In this frame, the x-axis is along the velocity vector of the spacecraft, the y-axis is along the orbit normal (radius cross velocity), and the z-axis completes the orthogonal triad.

$$\begin{aligned} X &= \vec{V} \\ Y &= \vec{R} \times \vec{V} \\ Z &= X \times Y \end{aligned}$$

Figure 7. VNC Coordinates

The real computational strength within Astrogator lies in the targeting sequence, which allows the definition of maneuvers in terms of goals to achieve. The basic targeting problem is: given a set of orbital goals, how can the control parameters be perturbed (and solved) to meet them? Astrogator uses a differential corrector process to iterate to a solution. Determining libration orbit insertion trajectories often requires multiple phased targeting segments where the goals define the intended orbits and the control parameters are the velocity change components and other transfer orbit characteristics.

### 2003 Direct Insertion into L1 Large Amplitude Lissajous Orbit

The original study by Pernicka, et al, was a system level analysis with some simplifying assumptions. It used co-planer transfer trajectories and circular orbits to determine C3 energy and orbit insertion  $\Delta V$  requirements for a 2003 Sun-Mars Lissajous communications relay concept. (Note: C3 is defined as negative the gravitational parameter of the central body divided by the semi-major axis. For hyperbolic orbits this is the square of the hyperbolic excess velocity.) That original data was generated with simplified force models and direct transfer to an orbit about L1. Our study used STK / Astrogator and the targeting process described in detail in the subsequent section to reproduce a subset of this data for three different times of flight (TOF) for closer analysis. No Z amplitude specifications were considered for these scenarios. A screen capture of the trajectory from the STK output is shown in Figure 8, where the view is of the XY plane looking in the  $-Z$  direction, using a Sun-Mars rotating coordinate frame. We found some agreement between the resulting data, which is presented in the table that follows.

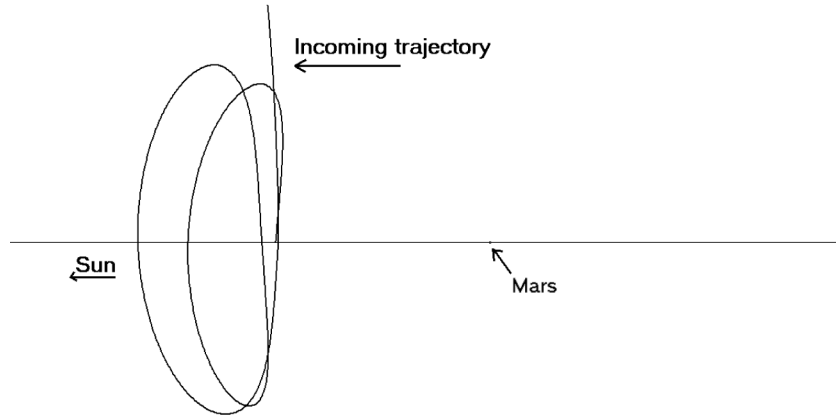


Figure 8. L1 Orbit Direct Insertion

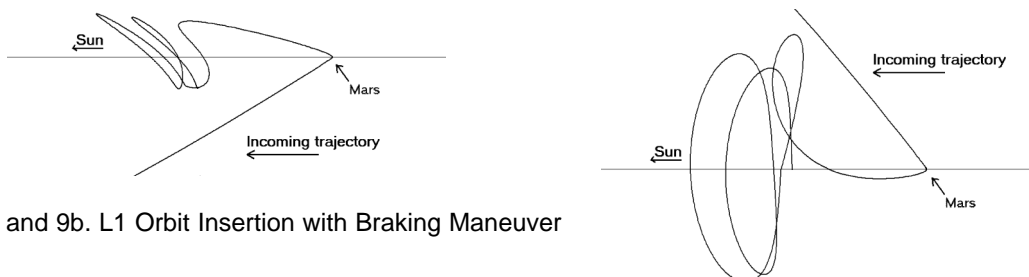
Table 1. Summary of Direct Transfer to L1 Lissajous; 13 Jun 03 Departure

| TOF (days) | C3 Energy (km <sup>2</sup> /sec <sup>2</sup> )<br><i>Original Study</i> | C3 Energy (km <sup>2</sup> /sec <sup>2</sup> )<br><i>Full Force Model</i> | Orbit Insertion Δv (km/sec)<br><i>Original Study</i> | Orbit Insertion Δv (km/sec)<br><i>Full Force Model</i> |
|------------|-------------------------------------------------------------------------|---------------------------------------------------------------------------|------------------------------------------------------|--------------------------------------------------------|
| 170        | 8.561                                                                   | 9.553                                                                     | 1.604                                                | 2.807                                                  |
| 200        | 7.910                                                                   | 8.883                                                                     | 1.196                                                | 2.425                                                  |
| 240        | 7.986                                                                   | 14.218                                                                    | 1.747                                                | 3.400                                                  |

The differences in C3 energy and ΔV are most likely due to the differences in the model parameters of the studies. This study used full force models, non-circular and non-coplanar transfers, and direct computation of the orbit insertion ΔV. Based on inspection of the Mars arrival trajectories, use of actual non-coplanar, eccentric planetary orbits seems to be a major factor. The data trends are still evident, however: the 200 day TOF case provides the minimum C3 energy and orbit insertion values (for the cases studied) and the longer and shorter duration flights require more energy and velocity change. Thus, for a 2003 mission (a baseline comparison year to be compatible with the original study) we provide this refined transfer data from our simulations with full-force models and non-coplanar, eccentric orbits. With these mission scenarios developed, more extensive simulation and analysis for various transfer parameters could be undertaken.

**2003 Transfer with Braking Maneuver at Mars Periapses**

Based on a helpful suggestion by Chauncey Uphoff, and some historical approaches identified by Dave Dunham, we investigated the use of a braking maneuver at close approach to Mars to lower the ΔV required for the Lissajous orbit insertion maneuver. This added a segment to the trajectory design and required some careful targeting for a close swingby and braking maneuver around Mars (targeting details are discussed in the next section of the paper). We modeled and simulated the 200 day TOF case for the 2003 mission to L1 with the braking maneuver, shown in Figures 9a (looking edge-on at the XZ plane) and 9b (looking down on the XY plane). The data and a comparison to the direct insertion case are presented in the table below.



Figures 9a and 9b. L1 Orbit Insertion with Braking Maneuver

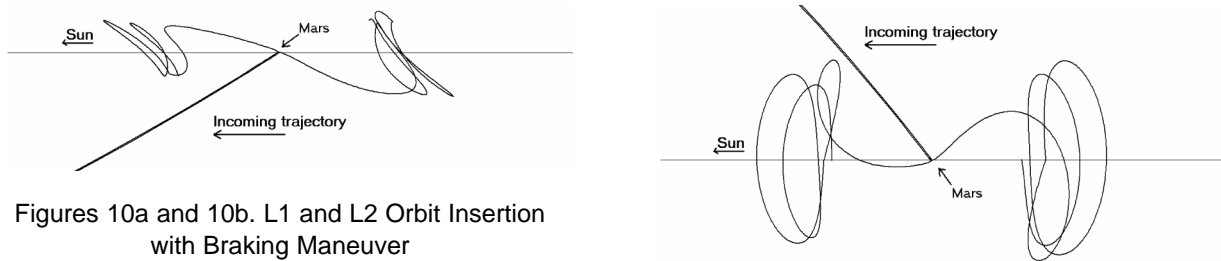
Table 2 Comparison of 2003 Transfers to L1 Orbit; 200 Day TOF

| Scenario         | C3 Energy (km <sup>2</sup> /sec <sup>2</sup> ) | Braking Δv (km/sec) | Orbit Insertion Δv (km/sec) | Total Δv (km/sec) |
|------------------|------------------------------------------------|---------------------|-----------------------------|-------------------|
| Direct Injection | 8.883                                          | 0                   | 2.425                       | 2.425             |
| Braking Maneuver | 9.056                                          | 0.856               | 0.104                       | 0.960             |

The braking maneuver resulted in a ΔV savings of 1.465 km/sec, which would lead to fuel mass savings and/or increase in payload capacity. This type of maneuver seems promising as a ΔV conserving technique, and so we adopted it for the other mission simulations that follow. However, there is plainly room for future investigations into the applicability of this trajectory for various mission profiles.

**2016 Transfer Braking Maneuver**

In order to provide data from this study that may aid future mission planners or lead to further research, we modeled a 2016 mission to place two vehicles in orbit about L1 and L2. We simulated a 200 day TOF as a baseline, as well as a 181 day TOF which, along with the departure date of 20 Feb 2016, was inspired by a JPL Ballistic Earth-Mars Trajectory study.<sup>17</sup> These trajectories are depicted in Figures 10a and 10b and relevant data is shown in the two tables which follow.



Figures 10a and 10b. L1 and L2 Orbit Insertion with Braking Maneuver

Table 3. Comparison of 2016 Transfers to L1 Orbit for Different TOF

| TOF (days) | C3 Energy (km <sup>2</sup> /sec <sup>2</sup> ) | Braking Δv (km/sec) | Orbit Insertion Δv (km/sec) | Total Δv (km/sec) |
|------------|------------------------------------------------|---------------------|-----------------------------|-------------------|
| 181        | 8.847                                          | 2.314               | 0.047                       | 2.360             |
| 200        | 10.377                                         | 1.710               | 0.047                       | 1.757             |

Table 4. 2016 Transfers to L1 & L2 Orbits for 200 Day TOF

| Orbit | C3 Energy (km <sup>2</sup> /sec <sup>2</sup> ) | Mid-course Δv (km/sec) | Braking Δv (km/sec) | Orbit Insertion Δv (km/sec) | Total Δv (km/sec) |
|-------|------------------------------------------------|------------------------|---------------------|-----------------------------|-------------------|
| L1    | 10.377                                         | 0                      | 1.710               | 0.047                       | 1.757             |
| L2    | 10.377                                         | 0.001                  | 1.708               | 0.085                       | 1.795             |

Table 3 shows that a shorter TOF to Mars can be achieved with a lower C3 energy value, but that trajectory requires a larger braking maneuver than the longer transfer, to achieve the same mission orbit. This indicates that with these types of missions the lower energy transfer may not yield a lower braking and insertion ΔV specification.

Table 4 shows how two vehicles could start on the same transfer trajectory initially (as with a simultaneous launch) and the L2 vehicle targeted for it’s close approach via a small mid-course correction. The simulation method is explained further in the next section. The total TOF to Lissajous orbit insertion is different for each vehicle, which would assist in the phasing of the vehicles that is required for the communications relay system to maintain adequate coverage of Mars.

### Z Amplitude and $\Delta V$ Analysis

Since specific mission performance specifications will drive the Lissajous orbit shaping requirements, we performed some basic investigations into the relationship between the orbit Z amplitudes and the  $\Delta V$  needed for the braking and mission orbit insertion maneuvers. We examined the 2016 transfer to an L1 orbit for 200 day TOF, targeting various amplitude values. The trajectories were very sensitive to small changes in the maneuvers (see Figure 11, looking towards the Sun), and the results are summarized in Table 5 below. The C3 energy for all cases was kept constant at  $10.377 \text{ km}^2/\text{sec}^2$ .

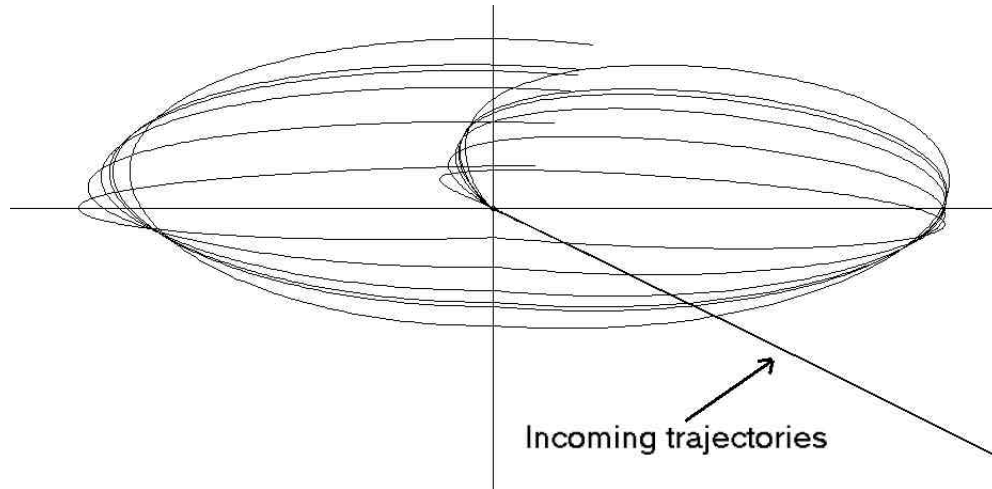


Figure 11. Orbits about L1 with Different Z Amplitudes

Table 5. 2016 Transfer to L1 Orbit with Varying Z Amplitude

| Z Amplitude (km) | Periapsis elevation (degrees) | Mid-course $\Delta v$ (km/sec) | Braking $\Delta v$ (km/sec) | Orbit Insertion $\Delta v$ (km/sec) | Total $\Delta \Delta$ (km/sec) |
|------------------|-------------------------------|--------------------------------|-----------------------------|-------------------------------------|--------------------------------|
| 50000            | -4.3                          | 0.00017                        | 1.71040                     | 0.04181                             | 1.75238                        |
| 100000           | -8.7                          | 0.00009                        | 1.71034                     | 0.04283                             | 1.75327                        |
| 140000           | -12.3                         | 0.00003                        | 1.71025                     | 0.04463                             | 1.75491                        |
| 160000           | -14.1                         | 0                              | 1.71019                     | 0.04595                             | 1.75614                        |
| 167447           | -14.7                         | 0                              | 1.71017                     | 0.04653                             | 1.75670                        |
| 200000           | -17.6                         | 0.00006                        | 1.71004                     | 0.04653                             | 1.75980                        |

The data from Table 5 demonstrate a correlation of the geometry of periapsis with the Z-amplitude. As a measure of the geometry, the elevation angle of the periapsis measured with respect to Mars’ orbit plane was used. Very slight changes in the elevation angle caused dramatic changes in the Z amplitude. (It was also noticed that the class of the Lissajous orbit could be changed by large variation of elevation angle, however this was not thoroughly investigated for this study.) As shown in the table, the mid-course correction  $\Delta V$  to change the elevation angle at periapsis is insignificant. Additionally, there is no significant change in the braking maneuver, leading to the conclusion that a wide range of Z amplitudes can be achieved with no fuel penalty.

### Relative Phasing Selection

As noted previously (see Figure 5), the key to obtaining sufficient communication coverage is to achieve 180 degree phasing of the two vehicles in their orbits. In other words, one is north of the Mars orbit plane while the other is south, and one is leading Mars while the other trails. The two-vehicle simulation from the sections above does not attempt to achieve the proper phasing for actual relay mission operations. This 180 degree phasing can be achieved by causing both spacecraft to reach their appropriate libration orbit insertion (LOI) points at the same time. In the above results with no phasing control, the “baseline scenario” shown in Figure 10 had an LOI time difference of 56 days.

Of course, each vehicle could be launched separately to achieve the proper phasing, but with very constrained launch windows. The redundant launch costs may also make that approach cost-prohibitive. This paper focuses on scenarios where both spacecraft are launched on the same launch vehicle. As a result, the relative phasing of the spacecraft in their Lissajous orbits is controlled by their onboard propulsion to affect LOI insertion time. Three possible methods were investigated: using a midcourse maneuver (as above), adjustment of TOF from periapsis Mars to LOI, and the use of a Martian phasing loop. All are discussed in the next section.

**Trajectories to Achieve Two-Vehicle Phasing**

The first method investigated to control the relative phasing was to use the mid course correction (MCC) maneuver 30 days after launch to change the time of arrival of the spacecraft at Mars. By adjusting the time of arrival, the time of insertion into the Lissajous orbit (the LOI maneuver) would also be changed.

The baseline scenario in Figure 10 shows that the trajectories arriving at Mars are not symmetric with respect to the Sun-Mars rotating coordinate system; the incoming trajectories arrive from the L1 side of Mars. A consequence of this is that the L1 spacecraft inserts before the L2 spacecraft reaches its insertion point. A first step in getting both spacecraft to arrive at their LOI points simultaneously was to adjust the L2 spacecraft trajectory so that it would arrive at the periapsis Mars point earlier than the L1 spacecraft. To do this, however, required a very large midcourse maneuver. In addition, the decreased time of flight caused the incoming velocity at Mars to increase, and changed the direction of the incoming asymptote, as shown in Figure 12 below. In that figure, the dashed line is the original baseline and the solid represents an earlier arrival at periapsis Mars.

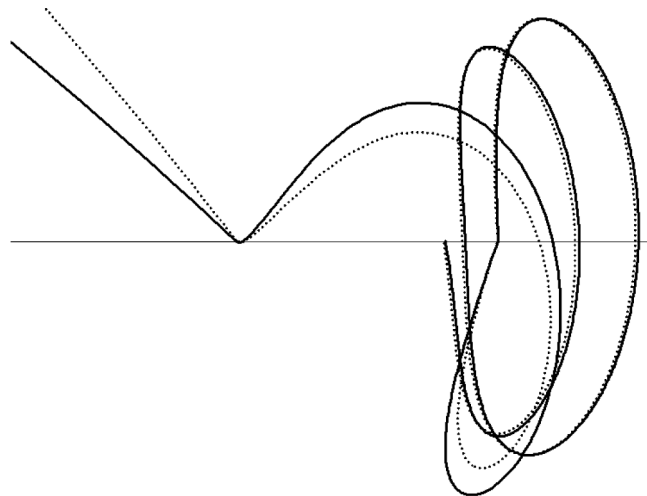


Figure 12. Mid-Course Maneuver Allows Earlier Periapsis Mars (solid line)

The change in the asymptote angle in turn caused the time of flight from periapsis Mars to LOI to increase, and the epoch of the LOI point did not vary the same as the change in periapsis Mars epoch. In fact, for the case examined, an earlier periapsis epoch resulted in a two day *delay* in LOI. In addition, the retrograde braking maneuver and the LOI  $\Delta V$  costs increased, again because of the change of the transfer trajectories. Table 6 shows the comparison data and the increase in  $\Delta V$ . This method proved unfeasible because of the large  $\Delta V$  cost associated with moving the epoch of LOI even a few days, and the direction of that movement for this case.

Table 6. Using MCC to Change Periapsis Date and Effect LOI Epoch

| Vehicle/case | MCC Mag (km/s) | Retro $\Delta V$ (km/s) | Periapsis Date | LOI Diff. from L1 Orig. (Days) |
|--------------|----------------|-------------------------|----------------|--------------------------------|
| L1 Original  | 0.00           | 1.71017                 | 7 Sep 2016     | 0.00                           |
| L2 Original  | 0.00129        | 1.70843                 | 7 Sep 2016     | 56.42                          |
| L2 -10 Days  | 0.281          | 2.00874                 | 28 Aug 2016    | 58.62                          |

The second method investigated to control phasing was to vary the time of flight of both vehicles from periapsis Mars to LOI. The time of flight is correlated with the amplitude, which is controlled by targeted B-dot-R value.<sup>22</sup> Thus, this TOF must be controlled to cause the L1 vehicle to insert later and have the L2 vehicle insert earlier so that their LOI times coincide. Our investigation results, detailed in the figures and Table 7 below, show that varying this TOF results in very large (and most likely unwanted) Lissajous orbit amplitudes (over 500,000 km) without achieving the synchronicity of the LOI required for the system phasing. However, there may be some applicability of this method to affect small changes in phasing if needed during operations.

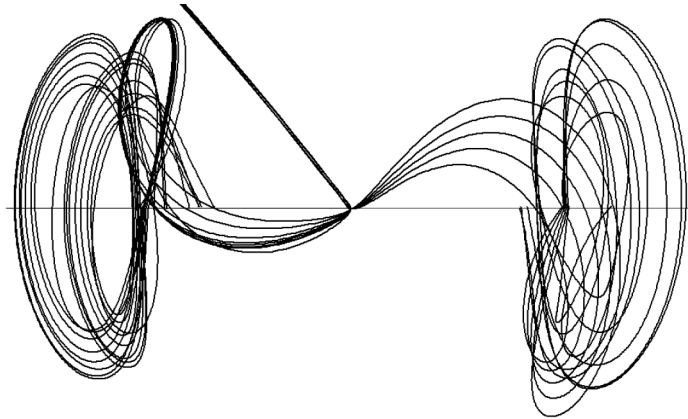


Figure 13a. Amplitude Variations Due to TOF Changes

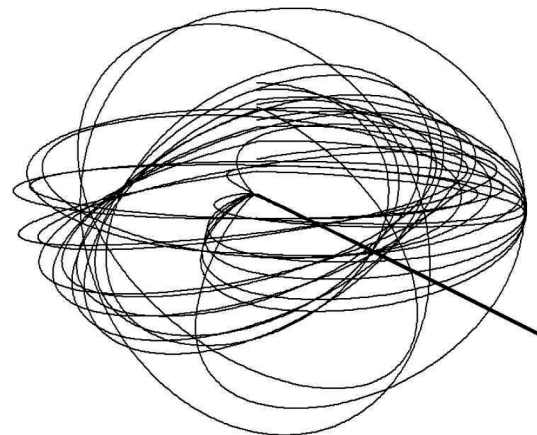
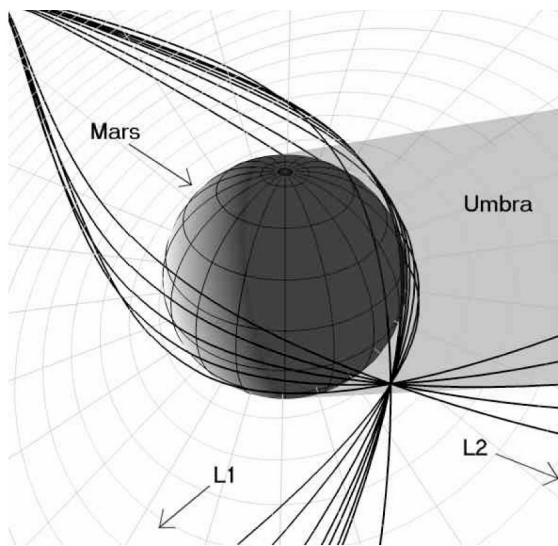


Figure 13c (above). Amplitudes About L1  
Figure 13b (left). Periapsis Mars

The third method to control phasing is the use of a phasing loop orbit about Mars prior to LOI. With this approach, the L2 vehicle performs its LOI maneuver after Mars swingby as in the baseline case and establishes the LOI time and phasing that the L1 vehicle must match. Using a retrograde capture maneuver at Mars periapsis, the L1 vehicle enters a phasing orbit about Mars. After one revolution in this orbit, a subsequent maneuver at periapsis transfers the vehicle out to the LOI point. The period of this phasing orbit summed with the time of flight of the transfer to LOI must be such that the desired epoch at LOI is achieved.

One might think that the phasing orbit period would be equal to the difference between LOI times for the L1 and L2 vehicles in the baseline configuration (56 days). However, since the phasing orbit periapsis point rotates in the Sun-Mars rotating frame, the transfer to LOI is longer than in the baseline scenario. Thus, to obtain the correct total TOF the phasing orbit period is shorter than expected. In fact, using a two-body orbit period calculation right after the capture maneuver set equal to the 56 day time difference actually causes a time delay far in excess of that required. The data

and figures below show these results. The use of a phasing orbit also introduces some flexibility into the execution of the entire mission. The result is that the 180 degree phasing of the two vehicles can be obtained. The results are below.

Table 7. Z-axis amplitude and LOI date as a function of Time of Flight (TOF)

| Transfer TOF (days) | Z-Amplitude at LOI (km) | Date of LOI          | LOI diff from L1 Orig. (Days) | Total $\Delta V$ (km/s) |
|---------------------|-------------------------|----------------------|-------------------------------|-------------------------|
| <b>L1 Transfers</b> |                         |                      |                               |                         |
| 184.39              | -167,106.57             | 10 Mar 2017 21:27:05 | 0.00                          | 1.7101691               |
| 188.77              | -66,257.64              | 15 Mar 2017 06:26:07 | 4.37                          | 1.7105497               |
| 194.64              | 68,229.80               | 21 Mar 2017 03:21:42 | 10.25                         | 1.7106852               |
| 198.28              | 153,862.98              | 24 Mar 2017 18:43:20 | 13.89                         | 1.7106055               |
| 199.98              | 195,445.37              | 26 Mar 2017 11:27:05 | 15.58                         | 1.7105053               |
| 201.92              | 244,697.19              | 28 Mar 2017 10:11:20 | 17.53                         | 1.7103805               |
| 203.05              | 273,937.27              | 29 Mar 2017 13:13:34 | 18.66                         | 1.7102926               |
| 212.70              | 529,029.71              | 8 Apr 2017 04:46:19  | 28.31                         | 1.7090500               |
| <b>L2 Transfers</b> |                         |                      |                               |                         |
| 228.67              | 715,548.91              | 24 Apr 2017 04:07:05 | 44.28                         | 1.7082738               |
| 230.62              | 542,729.85              | 26 Apr 2017 02:50:37 | 46.22                         | 1.7090732               |
| 234.91              | 381,369.62              | 30 Apr 2017 09:50:30 | 50.52                         | 1.7094752               |
| 240.82              | 235,000.62              | 6 May 2017 07:38:06  | 56.42                         | 1.7097184               |
| 248.62              | 100,106.83              | 14 May 2017 02:49:45 | 64.22                         | 1.7096993               |

Table 8. Phasing Loop Used to Equate LOI Epochs

| Vehicle/case    | Retro $\Delta V$ (km/s) | Phasing Loop Maneuver (km/s) | LOI Diff. From L2 Orig. (Days) | Total $\Delta V$ (km/s) |
|-----------------|-------------------------|------------------------------|--------------------------------|-------------------------|
| L1 Original     | 1.71017                 | 0.00000                      | 56.42                          | 1.71017                 |
| L1 Phasing Loop | 1.71656                 | 0.00933                      | 0.01                           | 1.72589                 |
| L2 Original     | 1.70843                 | 0.00000                      | 0.00                           | 1.70972                 |

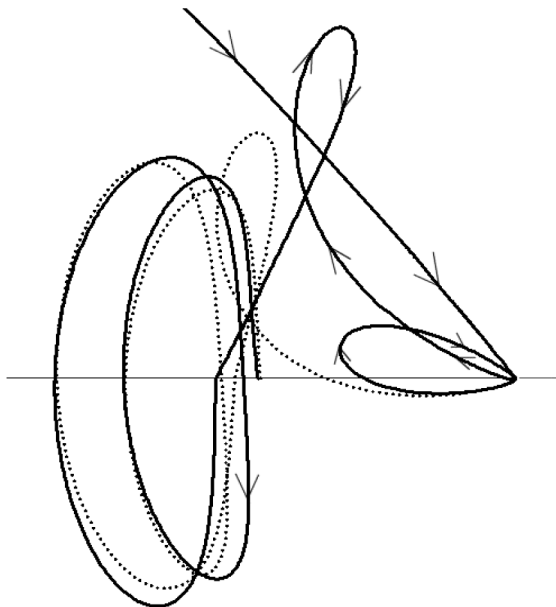


Figure 14a. Phasing Loop Trajectory(Solid)

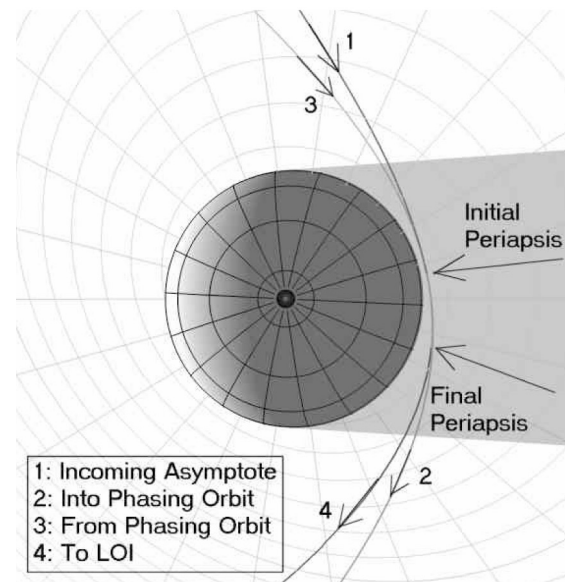


Figure 14b. Periapsis View

**Estimation of Communication Coverage Achieved**

Previous work has indicated that the 180 degree offset phasing of this communication system will allow near continuous coverage of the Martian surface so that exploration missions there would only experience communications loss for a few minutes twice a day, at the most. In order to verify and uncover more details on this, we analyzed the baseline 180 degree phased trajectories using the STK / Coverage module.

Two metrics were used to quantify the quality of coverage: “Maximum Revisit Time” and “Number of Gaps.” Gaps are the times on the surface of Mars that are not within line-of-sight of either satellite. Maximum Revisit Time is defined as the maximum duration of the gap in coverage over the entire coverage interval, which starts at LOI and goes for 674 Earth days (over one Martian year). “Number of Gaps” are the number of times in this same interval that contact cannot be made with at least one of the satellites. This was measured along one longitude line at 10 degree intervals of latitude.

This analysis approach takes into account the rotation of Mars and its tilt, using fully integrated trajectories phased via the method in the proceeding section. Table 9 shows tabular results for one particular epoch. For the mid-latitude regions, the gaps in coverage are about a half an hour, with one to two gaps per day. As a special note, the south polar region had the longest revisit times (6 days), which occurred 4 times during the year. By inspection, it seems that there may be a seasonal variation that should be investigated because of the effect near the poles. A complete investigation would include LOI epochs at various times of the Martian year and consider all locations on the planet.

Table 9. Summary of Coverage Analysis

**Targeting Methods Using STK / Astrogator<sup>1</sup>**

In this section we provide more detail on using the simulation and analysis tools which generated the results of the previous section. The transfer from the Earth to a Mars Lagrange orbit was targeted in a series of steps. The purpose of the targeting was to determine the control variables necessary to achieve this transfer. The initial orbit state represented the post launch Earth-centered hyperbolic trajectory. This was specified in target vector form, in the Earth-centered mean ecliptic and equinox of J2000 coordinate system. The seven parameters of the target vector are: epoch, radius of periapsis, C3 energy, right ascension (RA) and declination (Dec) of the outgoing hyperbolic asymptote, the velocity azimuth at periapsis, and the true anomaly.

For this study, the epoch was chosen to match previous work, the true anomaly was set to zero, the velocity azimuth set to 90 degrees, and the radius of periapsis set to 6678.0 km. This represents a satellite near the Earth at perigee. The remaining parameters, C3 energy and the direction of the trajectory (RA and Dec of the asymptote) were used as control parameters. Two methods of insertion into Lagrange orbits were utilized and are discussed separately below.

**Direct Transfer to L1 Lagrange Orbit**

For the direct transfer from Earth to the L1 Lagrange orbit, the control parameters were adjusted using a differential corrector technique to achieve three constraints at the point the trajectory crossed the ZX plane of Sun-Mars rotating libration-point coordinate system (this is the plane containing the Sun-Mars line and perpendicular to Mar’s orbit plane). The three constraints are the desired epoch of arrival, and the X and Z positions in the Sun-Mars rotating libration-point coordinates. This is shown in the figure below.

| Latitude (deg) | Max Revisit Time (hrs) | Number of Gaps |
|----------------|------------------------|----------------|
| 90.0           | 0.000                  | 1              |
| 80.0           | 3.639                  | 61             |
| 70.0           | 5.117                  | 335            |
| 60.0           | 3.499                  | 584            |
| 50.0           | 1.707                  | 902            |
| 40.0           | 0.696                  | 890            |
| 30.0           | 0.494                  | 846            |
| 20.0           | 0.441                  | 785            |
| 10.0           | 0.463                  | 733            |
| 0.0            | 0.486                  | 688            |
| -10.0          | 0.512                  | 649            |
| -20.0          | 0.543                  | 609            |
| -30.0          | 0.650                  | 574            |
| -40.0          | 0.845                  | 524            |
| -50.0          | 1.210                  | 491            |
| -60.0          | 5.994                  | 436            |
| -70.0          | 5.729                  | 237            |
| -80.0          | 7.425                  | 130            |
| -90.0          | 148.645                | 3              |

| Stage | Controls                            | Constraints                     | Dimension |
|-------|-------------------------------------|---------------------------------|-----------|
| I     | C3<br>Targ.Vec. RA<br>Targ.Vec. Dec | Epoch<br>$X_{RLP}$<br>$Z_{RLP}$ | 3x3       |

Figure 15. Direct Transfer Targeting

Once the desired time and position was achieved, the three components of the Lagrange-orbit insertion maneuver (LOI) was targeted as an impulsive  $\Delta V$  maneuver in four steps. First, LOI was targeted to achieve somewhat ideal velocity components for the Lissajous orbit at this point. Velocity in the X and Z rotating libration point directions were targeted to zero. Velocity in the Y direction was targeted to -0.16 km/sec (a representative value from previous analysis). Second, the LOI maneuver was corrected so that after propagating the trajectory a half revolution to the first ZX plane crossing, the X component of velocity ( $V_x$ ) would be zero (this represents a perpendicular plane crossing when projected into the XY plane, and is the same energy balancing technique mentioned by Dunham and Roberts<sup>14</sup>). After achieving the first ZX plane crossing, the third and fourth steps were to correct the LOI maneuver to achieve  $V_x$  of zero at the second, and then the third ZX plane crossings. The figure below illustrates this process.

| Stage | Controls                                                    | Constraints                                         | Dimension |
|-------|-------------------------------------------------------------|-----------------------------------------------------|-----------|
| I     | $\Delta V_{LOIv}$<br>$\Delta V_{LOIn}$<br>$\Delta V_{LOIc}$ | Post LOI:<br>$V_{xRLP}$<br>$V_{yRLP}$<br>$V_{zRLP}$ | 3x3       |
| II    | $\Delta V_{LOIv}$                                           | 1 <sup>st</sup> XZ Plane Cross:<br>$V_{xRLP} = 0$   | 1x1       |
| III   | $\Delta V_{LOIv}$                                           | 2 <sup>nd</sup> XZ Plane Cross:<br>$V_{xRLP} = 0$   | 1x1       |
| IV    | $\Delta V_{LOIv}$                                           | 3 <sup>rd</sup> XZ Plane Cross:<br>$V_{xRLP} = 0$   | 1x1       |

Figure 16. Direct LOI Targeting

### Transfer Using Braking Maneuver at Mars Periapsis

The transfer to a Mars Lagrange point orbit using a braking maneuver at the close approach at Mars before the LOI maneuver was also targeted in stages. First, the target vector control parameters were adjusted by the differential corrector to achieve an epoch at periapsis Mars, and B-Plane components to place the trajectory on the anti-Sun side of Mars. Since this stage is just a first guess, the values used were B-dot-T of -10,000 km, and B-dot-R of 0.0 km. The entire sequence is shown in the figure and explained further below.

The second step refined this to the desired close approach conditions. Using the same control parameters, the radius of close approach was used instead of B-dot-T, and was targeted to a radius of 3,600 km (about 200 kilometers altitude).

After the constraints at periapsis were met, the magnitude of a retrograde braking maneuver (anti-velocity direction) was used at periapsis to shape the trajectory until the trajectory crossed the XZ plane at the desired X distance in the Sun-Mars rotating libration-point coordinate system ( $X_{RLP}$ ). After the retrograde maneuver was calculated, the LOI maneuver was planned using the same 4-step method previously described for the direct transfer.

The transfer to the L2 Lagrange orbit was planned in a similar manner, except that the trajectory must pass on the Sunward side of Mars at the close approach. This was done using a mid-course correction (MCC) maneuver as a control

parameter, which also allowed the initial transfer parameters to be the same for both the L1 and L2 vehicles. Some additional graphic explanation of B-plane targeting is shown in the figures below, and further detail can be found on the STK web site.<sup>26</sup>

| Stage    | Controls                            | Constraints                                         | Dimension |
|----------|-------------------------------------|-----------------------------------------------------|-----------|
| I        | C3<br>Targ.Vec. RA<br>Targ.Vec. Dec | Periapsis Epoch<br>B·T<br>B·R                       | 3x3       |
| II       | C3<br>Targ.Vec. RA<br>Targ.Vec. Dec | Periapsis Epoch<br>B·R<br> R <sub>p</sub>           | 3x3       |
| III      | $\Delta V_{\text{retro}}$           | 1 <sup>st</sup> XZ Plane Cross:<br>X <sub>RLP</sub> | 1x1       |
| IV - VII | Same as LOI                         | Same as LOI                                         | 3x3, 1x1  |

Figure 17. LOI Using a Braking Maneuver

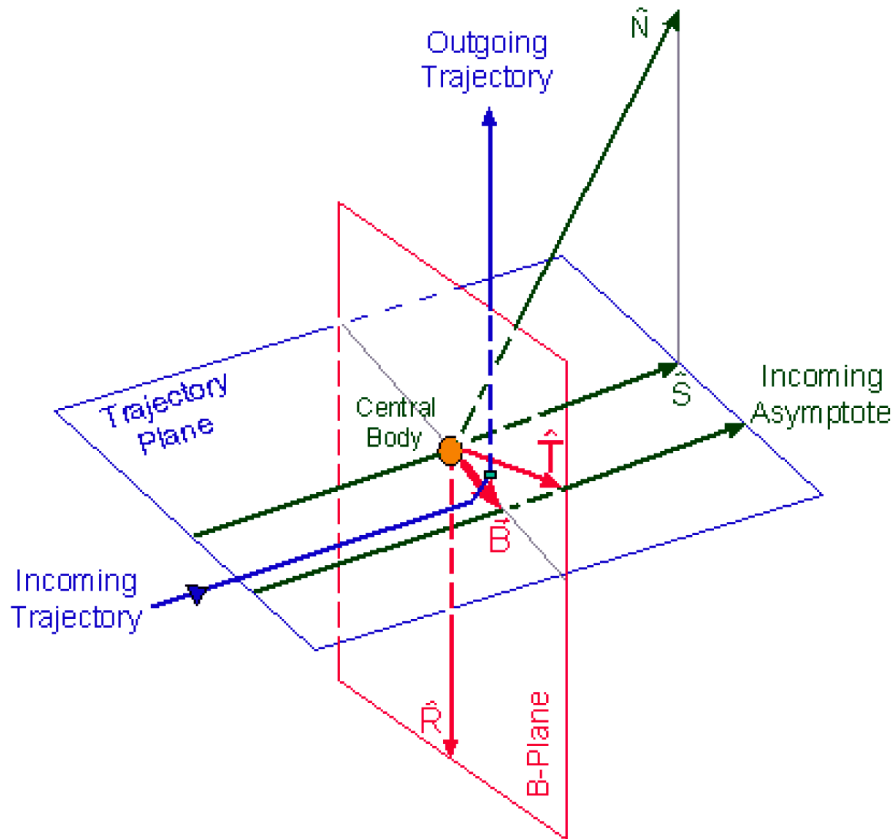


Figure 18. B-Plane Targeting<sup>27</sup>

### Transfer Using Braking Maneuver to Achieve Desired Z Amplitude

The concept for targeting a desired Z amplitude for the Lagrange orbit is analogous to the technique using Earth's moon as described by Sharer, et al.<sup>21</sup> The Z amplitude can be directly controlled as a function of the position of the trajectory as it passes through its close approach to Mars. The process is outlined in the figure and described below.

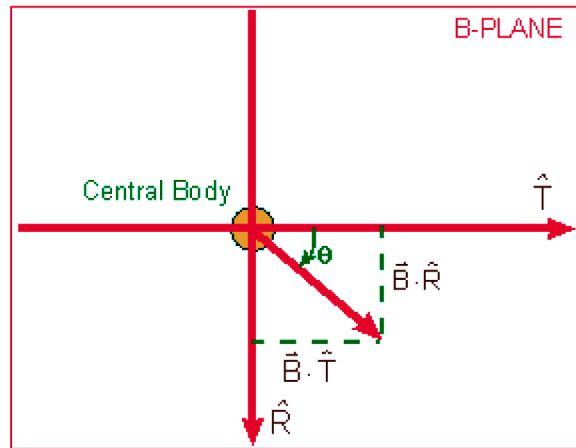


Figure 19. The B-Plane<sup>27</sup>

| Stage    | Controls                                                                          | Constraints                                                                             | Dimension |
|----------|-----------------------------------------------------------------------------------|-----------------------------------------------------------------------------------------|-----------|
| I        | $\Delta V_{MCCx}$<br>$\Delta V_{MCCy}$<br>$\Delta V_{MCCz}$                       | Periapsis Epoch<br>B·T<br>B·R                                                           | 3x3       |
| II       | $\Delta V_{MCCx}$<br>$\Delta V_{MCCy}$<br>$\Delta V_{MCCz}$                       | Periapsis Epoch<br>B·R<br>$ R_p $                                                       | 3x3       |
| IIa      | Adjust B·R to get approximate $Z_{RLP}$ ; repeat stage II                         |                                                                                         |           |
| III      | $\Delta V_{retro}$                                                                | 1 <sup>st</sup> XZ Plane Cross:<br>$X_{RLP}$                                            | 1x1       |
| IV       | $\Delta V_{MCCx}$<br>$\Delta V_{MCCy}$<br>$\Delta V_{MCCz}$<br>$\Delta V_{retro}$ | Periapsis Epoch<br>$ R_p $<br>1 <sup>st</sup> XZ Plane Cross:<br>$X_{RLP}$<br>$Z_{RLP}$ | 4x4       |
| V - VIII | Same as LOI                                                                       | Same as LOI                                                                             | 3x3, 1x1  |

Figure 20. Targeting Z-Amplitude Variations

The initial targeting is the same B-Plane targeting described above: first B-dot-T and B-dot-R, and then B-dot-R and Radius of periapsis. The initial target vector parameters were not used at this step because the corrections to the parameters were too small, being on the order of a double precision number. Instead, a MCC maneuver was used 30 days after Earth departure.

After the epoch, B-plane, and radius of periapsis constraints were achieved, the retrograde braking maneuver was targeted to achieve as described above. Then the Z distance (amplitude) was checked, and if it was significantly far from the desired value, the previous step was repeated with a different B-dot-R value. (B-dot-R is directly related to the elevation of periapsis with respect to the Mars' orbit plane.)

The next stage involved targeting the four constraints that must be simultaneously met: the epoch at periapsis, the radius of periapsis (to prevent the trajectory from hitting Mars), the X position at LOI, and the Z amplitude. In addition to the three components of the MCC maneuver, the magnitude of the braking maneuver was also used as a control.

Once this step converged, the LOI maneuver was targeted using the same 4-step method described above for the direct insertion.

### Transfer to Achieve Relay Phasing

The first two methods attempted to control phasing used the approaches described above. The 3<sup>rd</sup> method, which utilized a phasing loop for the L1 satellite, required a modified targeting procedure. The capture maneuver was targeted such that after one phasing loop and then subsequent transfer to LOI, the epoch of LOI would match the epoch of the L2 satellite LOI. In order to achieve this, two differential corrector targeting schemes were employed simultaneously. An inner targeter calculated the maneuver magnitude in the velocity direction needed to transfer from the phasing orbit to the Lissajous orbit. This inner targeter was “wrapped” by an outer targeter which calculated the retrograde maneuver at the first Mars periapsis. This targeter was set up to adjust the maneuver magnitude to achieve the epoch at LOI which occurs after the inner targeter has converged on a solution. Therefore, each time the outer targeter iterated and searched for the capture maneuver, the inner targeter was re-run to calculate the transfer from the phasing orbit to LOI.<sup>23</sup>

### Station-keeping

Due to the precarious nature of the Lissajous orbit, precise and continuous station-keeping (SK) techniques must be employed. Additionally, the precision required for certain missions located around the Sun-Mars Lagrange points requires the fidelity of such SK maneuvers to be extremely high. Historical data and studies indicate that SK  $\Delta V$ s as little as 1 mm/sec could be required.

Station-keeping techniques fall into two major categories.<sup>14</sup> The first, referred to as a “tight” control technique, attempts to target the vehicle back to a nominal three-dimensional path. The second is the “loose” control technique that uses a simpler “orbital energy balancing” strategy to closely mirror a Lissajous orbit. The two control techniques differ only in the number of  $\Delta V$  components that are varied. The loose technique will simply vary one component of  $\Delta V$  while the tight technique varies two or more to achieve a nominal Lissajous orbit.

### History<sup>14,18</sup>

The third International Sun-Earth Explorer (ISEE-3) flown to the Sun-Earth L1 point in 1978 used the tight control technique in an attempt to maintain its trajectory as close to a nominal halo orbit as possible. This mission, being the first to orbit a Sun-Earth libration point, had the luxury of a large supply of fuel to allow for uncertainties in the insertion to and maintenance of the new orbit. The relatively small errors encountered during insertion into the halo orbit left a large amount of fuel that could be used specifically for station-keeping. Over the four years that ISEE-3 was established at the L1 point, 15 SK maneuvers were performed totaling 30.06 m/sec at an average of 2.00 m/sec per maneuver. The time between the maneuvers averaged 82 days.

While the large amount of fuel planned for the ISEE-3 mission allowed for very tight control of its halo orbit, a more optimal SK method was planned for the Solar Heliospheric Observatory (SOHO). Prior to its establishment at the Sun-Earth L1 point in 1996, SOHO mission planners sought ways in which to decrease its SK costs. If the complexity of SK maneuvers for SOHO could be dramatically reduced, or “loosely” controlled, the fuel load, and therefore costs, could be also be reduced. In the “orbital energy balancing” technique that evolved, only one component of  $\Delta V$ , in this case the x-component, would be varied. The result of this simplification achieved a threefold reduction in SK costs from roughly 7.5 m/sec per year for ISEE-3 to less than 2.3 m/sec per year for SOHO.

The major drawback with the loosely controlled technique used on SOHO was that it did not maintain a periodic halo orbit *precisely*. The resultant orbit was, however, a Lissajous path that mirrored the nominal halo orbit so closely that for all practical purposes it could be considered equivalent. The loose control technique was therefore proven as an effective means of achieving lower SK costs when precise orbit mapping was not necessary.

### Station-keeping for the Sun-Mars Lissajous Orbits

For future missions to Mars using the Sun-Mars Lagrange points, mission planners will have to consider several factors prior to making a decision on the SK technique to be used. Obviously mission requirements will dictate whether the loose control technique can be used to optimize SK costs or if the higher precision of the tight technique is necessary.

In our example of a communication system in orbits about the Mars system example, the timing of SK burns is critical so as to prevent unexpected and inconvenient losses in communications coverage to the users on the Martian surface. One solution to such a problem is to overlap the SK maneuvers with the spacecraft's preplanned attitude and momentum adjustments. This allows the attitude control, momentum management, and SK maneuvers to complement one another and minimizes the down time of the system. Dunham and Roberts have shown that for any  $\Delta V$  error, the SK that follows is also minimized. If, however, the insertion  $\Delta V$  error is greater than that expected the magnitude of the SK maneuvers will increase and the SK costs will rise.

The second factor in SK frequency determination is the effect that subsequent SK burns have on the overall orbit error. This can be further broken down to the actual magnitude of the orbit error at the end of the last burn, the time since that burn, and the accuracy of the burn itself as executed. Obviously, this orbit error will increase with time and the larger the error, the sooner a subsequent burn will need to be performed. The key here is to minimize the magnitudes of the burns.<sup>14</sup>

Once the frequency and magnitude of the required SK maneuvers are determined, the optimal timing of such maneuvers will need to be considered. For the communications system example, the timing of SK burns is critical so as to prevent unexpected and inconvenient losses in communications coverage to the users on the Martian surface. One solution to such a problem is to overlap the SK maneuvers with the spacecraft's preplanned attitude and momentum adjustments. This allows the attitude control, momentum management, and SK maneuvers to complement one another and minimizes the down time of the system.

Dunham and Roberts have shown that small  $\Delta V$  errors on order of 0.1 mm/sec for the Sun-Earth / Moon system cause noticeable deviation from the nominal after about three revolutions in the Lissajous orbit.<sup>14</sup> In our study, the same error was applied to the Sun-Mars L1 Lissajous orbit as shown in Figure 21. This error caused noticeable deviations after only one and a half revolutions. However, because the period of the Mars Lissajous is about twice that of the Earth Lissajous, the deviations occur approximately after the same duration in time. This is an indicator that the station-keeping requirements for the Mars Lissajous will be on the same order as seen for the Earth missions, in terms of fuel used per year. Of course, a thorough error analysis study could be made later to prove this, accounting for the errors and uncertainties.

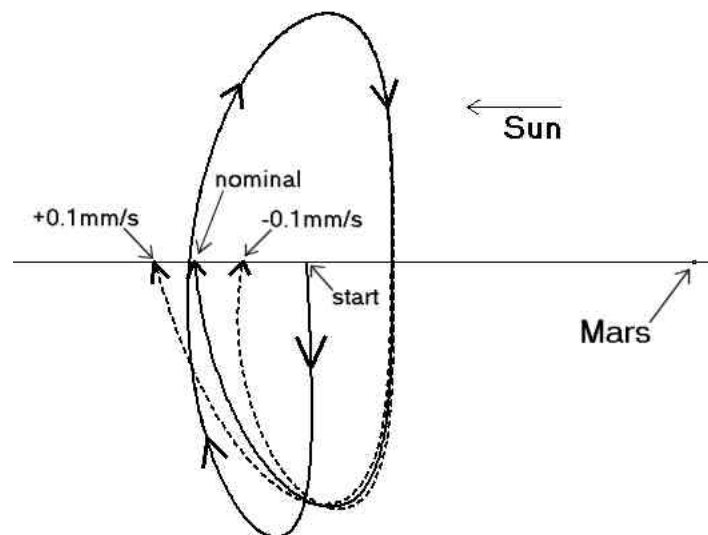


Figure 21. Effect of small errors on Lissajous orbit

Further research for this study explored the station-keeping sensitivities of spacecraft in these orbits via Monte Carlo analysis. The uncertainties included those due to the orbit determination process, possible change in the effective area of the spacecraft affecting the Solar radiation pressure acceleration, and possible errors in the station-keeping maneuver execution.

### Monte Carlo Simulation Approach

The uncertainties were modeled as uncorrelated errors. The uncertainty magnitudes were: 100 meters in position, 10 cm/second in velocity, 10% uncertainty in the area of the spacecraft (which could represent attitude changes), and a  $\Delta V$  error of 10 cm/second (These could be attributed to both errors in execution of station-keeping maneuver and attitude thruster control effects). A Monte Carlo simulation was setup to randomly vary these eight parameters and propagate the baseline L2 trajectory for 90 days. A station-keeping maneuver was then targeted at that time to return the trajectory to that of a periodic orbit for the remainder of the Martian year. The statistics were gathered on the magnitude of the station-keeping maneuver required to correct the trajectory.

The results of the Monte Carlo simulation with 100 runs yielded an average station-keeping  $\Delta V$  magnitude of 0.044 m/s (with standard deviation of 0.003). The same simulation was run for a large amplitude L2 orbit in the earth system (for comparison) and the average  $\Delta V$  was 0.45 m/s and standard deviation of 0.03. Since the period of the Earth is approximately half that of Mars, a second Earth-centered L2 Monte Carlo run was made where the station-keeping maneuver was done after only 45 days of propagation. The average  $\Delta V$  was 0.43 m/s with the same standard deviation. These results seem to indicate that the Martian Lissajous orbits require an order of magnitude less station-keeping  $\Delta V$  than those in the Earth system. One possibility for this that was considered is Lunar effects; but the examination of a Lissajous about L2 of the Sun-Earth system with the moon removed from the model yielded no significant difference in results. There are several other possibilities to be explored, including the different distances from the Sun and planet sizes.

### Conclusions<sup>22,23</sup>

This research began by re-examining a 2-vehicle communication relay system orbiting the Sun-Mars libration points, including transfer orbits, injection strategies, and station-keeping, to see how past studies and data compared to that from current desktop computing techniques using full-force model targeting and propagation (namely, the Satellite Tool Kit (STK) / *Astrogator* module). Earth-Mars transfers and Lissajous orbit injections for a 2016 mission were analyzed. It was found that trajectory trends from the previous studies were still valid when using full force models, however the actual magnitudes of the maneuvers could increase. This work also highlights the fact that the minimum departure C3 energy does not always correspond to the minimum LOI maneuver. Also revealed was that using a braking maneuver at a low altitude (200 km) Mars periapsis prior to LOI saves significant spacecraft on-board fuel, for certain approach trajectories. One can take advantage of the geometry of this close approach to control the Z amplitude and class of the Lissajous orbit as well. It was also determined that the loose control technique for station-keeping could be appropriate for the L1 and L2 communication relay concept. The stability of these orbits are on the same order as the Sun-Earth orbits in terms of deviations from nominal as a function of time.

Three methods were explored to achieve the 180 degree relative phasing of the spacecraft in their respective Lissajous orbits:

1. Adjusting the time of arrival at Mars periapsis using a midcourse correction;
2. Adjusting the time of flight from periapsis Mars to LOI by altering the amplitude of the Lissajous orbit; and
3. The addition of a phasing loop before the transfer to L1.

The first method proved too costly in terms of  $\Delta V$ . The second method did not move the LOI epochs close enough together. The third method was successful, and the targeting algorithm was described.

The quality of coverage was investigated using the fully numerically integrated trajectories and the actual motion of Mars' polar axis. For most latitudes, the maximum gap was found to be about a half an hour, which is slightly longer than previous papers suggested, but still within the scope of the missions described. The poles behave somewhat differently, with longer gaps, but far fewer. Future work could include investigation of the effect on coverage of orbit phasing with the Martian seasons.

An estimate of the station keeping cost for a Mars L2 orbit was calculated using a Monte Carlo technique, varying the initial orbit state, area, and maneuver execution errors. This was compared with a similar Earth L2 orbit, and the Mars

orbit requires about an order of magnitude less  $\Delta V$  for the maneuver. The reasons behind this are not fully understood, and could be pursued in future work.

Overall, the study has provided useful initial data on the trajectory designs to place vehicles in Lissajous orbits about the Sun-Mars L1 and L2 points, while showing that the innovative use of the two-satellite communication system is a practical concept for Mars exploration.

### Acknowledgments

The authors wish to thank Hank Pernicka and Chauncey Uphoff for their invaluable assistance with portions of this study. We also thank Bob Farquhar and Dave Dunham of the Applied Physics Laboratory at Johns Hopkins University for their correspondence and discussions on the topic. Thanks go as well to Professor Don Danielson and the Space Systems Academic Group at the US Naval Postgraduate School. Roger Martinez of AGI provided key support for the Mars Society presentation. We especially recognize Dean Rudy Panholzer at the US Naval Postgraduate School for his support of all the conference presentation efforts.

### References

1. J. Carrico et al., "Rapid Design of Gravity Assist Trajectories," Proceedings of the ESA Symposium on Spacecraft Flight Dynamics held in Darmstadt, Germany, 30 September - 4 October 1991 (ESA SP-326, December 1991).
  2. C.D. Brown, "Spacecraft Mission Design," AIAA Education Series, 1992, pp. 96-98.
  3. V.G. Szebehely, "Adventures in Celestial Mechanics," University of Texas Press, Austin Texas 1989.
  4. D.A. Vallado, "Fundamentals of Astrodynamics and Applications," McGraw-Hill, New York, 1997.
  5. D. Halliday, R. Resnick, J. Walker, "Fundamentals of Physics, Extended," John Wiley & Sons, New York, 1997.
  6. H. Pernicka, D. Henry, M Chan, "Use of Halo Orbits to Provide a Communication Link Between Earth and Mars," AIAA Paper 92-4584, 1992.
  7. V.G. Szebehely, "Theory of Orbits: The Restricted Problem of Three Bodies," Academic Press, New York and London, 1967.
  8. Website: [www.users.skynet.be](http://www.users.skynet.be), "The Guide to the Universe."
  9. K.C. Howell, "Families of Orbits in the Vicinity of the Colinear Libration Points," AIAA Astrodynamics Specialist Conference, Paper 98-4465, August 1998.
  10. Website: [www.map.gsfc.nasa.gov](http://www.map.gsfc.nasa.gov), "Microwave Anisotropy Probe."
  11. G. Gomez, K.C. Howell, J. Masdemont, C. Simo, "Station-Keeping Strategies for Translunar Libration Point Orbits," AIAA Spaceflight Mechanics Meeting, Paper 98-168, 1998.
  12. P. Keaton, "A Moon Base/Mars Base Transportation Depot," Los Alamos National Laboratory, LA-10552-MS, UC-34B, September 1985.
  13. E. Belbruno and J. Carrico, "Calculation of Weak Stability Boundary Ballistic Lunar Transfer Trajectories," AIAA/AAS Astrodynamics Specialist Conference, AIAA Paper 2000-4142, 14-17 August 2000.
  14. D. Dunham and C. Roberts, "Stationkeeping Techniques For Libration-Point Satellites," AIAA/AAS Astrodynamics Specialist Conference, AIAA Paper 98-4466, 10-12 August 1998.
  15. W. Kok-Fai Tai, "Mars Communication Network Design Trade Study," Master of Science Thesis, San Jose State University, 1998
  16. M. Danehy, "Martian Communications Network Design Trade Study," Master of Science Thesis, San Jose State University, December, 1997.
  17. S. Matousec and A. Sergeevsky, "Feasible Ballistic Earth to Mars Trajectories from 2002 to 2020," chart for Mars Surveyor Program Advanced Missions Studies Office, March, 1998.
  18. R. Farquhar, "The Flight of ISEE-3/ICE: Origins, Mission History, and a Legacy," AIAA Paper 98-4464, August 1998.
  19. R. Farquhar, "Stationkeeping in the Vicinity of Collinear Libration Points with an Application to a Lunar Communications Problem," AAS Science and Technology Series: Space Flight Mechanics Specialist Symposium, Vol. 11, pp. 519-535 (Presented in Denver, CO, July 1966).
  20. R. Farquhar, et al, "Trajectories and Orbital Maneuvers for the First Libration-Point Satellite," Journal of Guidance and Control, Vol. 3, No. 6, Nov-Dec, 1980, pp. 549-554.
  21. P. Sharer, J. Zsoldos, and D. Folta, "Control of Libration Point Orbits Using Lunar Gravity-Assisted Transfer," AAS-93-295, Spaceflight Dynamics 1993, Vol. 84, Part 1: Advances in the Astronautical Sciences, Proceedings of AAS/NASA symposium, April, 1993.
  22. J. Strizzi, J. Kutrieb, P. Damphousse, and J. Carrico, "Sun-Mars Libration Points and Mars Mission Simulations," AAS-01-159, February 2001.
  23. J. Carrico, J. Strizzi, J. Kutrieb, and P. Damphousse, "Trajectory Sensitivities for Sun-Mars Libration Point Missions," AAS-01-327, July 2001.
  24. R. Farquhar, "Future Missions for Libration-point Satellites," Astronautics and Aeronautics, May 1969.
  25. R. Farquhar, "Lunar Communications with Libration-Point Satellites," Journal of Spacecraft and Rockets, 1967.
  26. Website: [www.stk.com](http://www.stk.com)
  27. NASA, "Mission Analysis and Design Tool (Swingby): Mathematical Principles," Rev 1, Sept 1995 (Draft), Sect 4.4.1.
- Various on-line resources for some figure art.